Received: 6 June 2017 | Revised: 11 September 2017 | Accepted: 19 October 2017

DOI: 10.1002/sia.6355

WILEY SURFACE and INTERFACE ANALYSIS

RESEARCH ARTICLE

Dye degradation studies of Mo-doped TiO_2 thin films developed by reactive sputtering

M. Sreedhar[1] | J. Brijitta[1] | I. Neelakanta Reddy[2] | Migyung Cho[3] | Jaesool Shim[2] | Parthasarathi Bera[4] | Bhavana N. Joshi[5] | Sam S. Yoon[5]

[1] Centre for Nanoscience and Nanotechnology, Sathyabama University, Chennai 600119, India

[2] School of Mechanical Engineering, Yeungnam University, Gyeongsan, Gyeonsanbuk-do, 712-749, Republic of Korea

[3] Department of Game Engineering, College of Information and Communication, Tongmyong University, Busan, Republic of Korea

[4] Surface Engineering Division, CSIR–National Aerospace Laboratories, Bengaluru 560017, India

[5] School of Mechanical Engineering, Korea University, Seoul 02841, Republic of Korea

Correspondence Mi-Gyung Cho, Department of Game Engineering, College of Information and Communication, Tongmyong University, Busan, Republic of Korea
Email: mgcho@tu.ac.kr

Jaesool Shim, School of Mechanical Engineering, Yeungnam University, Gyeonsanbukdo 712-749, Gyeongsan, Republic of Korea
Email: jshim@ynu.ac.kr

Funding information
National Research Foundation of Korea (NRF), Grant/Award Number: 2015R1C1A2A01052256

TiO_2 thin films with various Mo concentrations have been deposited on glass and n-type silicon (100) substrates by this radio-frequency (RF) reactive magnetron sputtering at 400°C substrate temperature. The crystal structure, surface morphology, composition, and elemental oxidation states of the films have been analyzed by using X-ray diffraction, field emission scanning electron microscopy, atomic force microscopy, and X-ray photoelectron spectroscopy, respectively. Ultraviolet-visible spectroscopy has been used to investigate the degradation, transmittance, and absorption properties of doped and undoped TiO_2 films. The photocatalytic degradation activity of the films was evaluated by using methylene blue under a light intensity of 100 mW cm^{-2}. The X-ray diffraction patterns show the presence of anatase phase of TiO_2 in the developed films. X-ray photoelectron spectroscopy studies have confirmed that Mo is present only as Mo^{6+} ions in all films. The Mo/TiO_2 band gap decreases from ~3.3 to 3.1 eV with increasing Mo dopant concentrations. Dye degradation of ~60% is observed in Mo/TiO_2 samples, which is much higher than that of pure TiO_2.

KEYWORDS

band gap, dye degradation, Mo/TiO_2, thin film, transmittance

1 | INTRODUCTION

TiO_2 is one of the most effective semiconducting photocatalyst materials owing to its high chemical stability, nontoxicity, high catalytic activity, and low cost.[1] The high photocatalytic activity of TiO_2 is caused by photogenerated charge carriers (electrons [e^-] and holes [h^+]). The electrons actively participate in the reduction of molecular oxygen, and the holes mainly oxidize organic compounds. TiO_2 is also used in a wide variety of other industrial applications, such as self-cleaning materials, gas sensors, and solar energy conversion.[2-5] However, the efficiency of TiO_2 is limited by its wide band gap of ~3.4 eV (depending on the particle size and other properties) and high e^--h^+ pair recombination rate. Because of these drawbacks, TiO_2 can only generate e^--h^+ pairs and degrade organic compounds under ultraviolet light illumination. Thus, it is challenging to design a novel photocatalyst with a lower recombination rate and high activity under visible light.

Decreasing the optical band gap of TiO_2 by introducing the dopant ions is a well-known fact. However, it seems to be an important matter as, at the same time, not to create unwanted charge recombination centers and localized electronic states, which would prevent an effective charge separation of excited electron hole pairs. Additionally, an uncontrolled decreasing of conduction band may place the band edge below the O_2 affinity level, subsidize the formation of oxygen radicals, which are the key factors in photocatalytic reactions.[6] In spite of these potential problems, the effective way of decreasing the band gap of

M. Sreedhar and I. Neelakanta Reddy contributed equally to this work.

TiO_2 is by doping with cations that occupy substitutional positions of the network. The theoretical analysis shows that energy absorption decreases proportionally to the number of doping atoms. For a random distribution of substitutional atoms, a Gaussian-type density of states can appear at the valence or conduction bands.[7] The corresponding density of states is thus directly proportional to the number of doping ions, which gives a chance to manage visible light absorption. The balance between the above mentioned potential negative effect by the presence of localized electronic states and the positive effect in the band gap energy requires intense research and is essentially an open question.

Recently, numerous attempts have been made to decrease the band gap of TiO_2 by doping TiO_2 with metals and nonmetals like Fe,[8] La,[9] Ce,[10] N,[11,12] C,[13-15] and F.[16] Reducing the band gap of TiO_2 increases its absorption in the visible region, which leads to an increase in the overall photocatalytic efficiency. The dopant atoms delay e^--h^+ pair recombination and reduce the band gap of TiO_2. The microstructures and electronic structures of TiO_2 may also modify its photocatalytic efficiency. Doping with transition metals has been carried out extensively because of their unique *d* electron configurations and also fulfills the 2 primary conditions mentioned above.[17,18] TiO_2 has been doped with transition metals like Mo, Nb, and W, and these transition metal ions can either segregate on the surface of TiO_2 or be incorporated into the substitutional and interstitial sites of TiO_2. The substitution of dopants into different locations exerts various effects on the properties of TiO_2. However, substitutional dopant ions are the major contributor to changes in the electronic structure and absorption efficiency of TiO_2.[19]

Various techniques like sputtering, spin coating, sol-gel, and dip coating have been used to deposit doped TiO_2 thin films.[20-22] Table 1 summarizes details of literature available on molybdenum-doped TiO_2 films deposited by various techniques.[19,21,23-30] The table shows wide range of molybdenum concentrations in TiO_2 and its effect on degradation properties of dye.[19,21,23-30] Among all other techniques, sputtering technique is one of the best physical vapor deposition methods for producing thin films with high chemical stability and high adhesion and has been used to deposit TiO_2 and Mo-doped TiO_2 thin films. The transition metal Mo has been used as a dopant in this study because it shifts the absorption edge of TiO_2 into the visible region and enhances its photocatalytic efficiency.[28,31-33] Table 1 shows the influence of Mo doping on degradation efficiency of methylene blue (MB) and methyl orange. However, studies on the influence of Mo-doped TiO_2 deposited by radio-frequency (RF) reactive sputtering for photocatalytic applications are not systematic and unclear. Furthermore, optimizing the parameters to enable photocatalysts to work under visible light is likely to have significant technological benefits.

In this study, Mo/TiO_2 films were deposited on silicon and glass by using reactive RF sputtering at 400°C substrate temperature. The crystalline structure, morphology, elemental oxidation states, and optical properties of the Mo/TiO_2 thin films have been investigated. Moreover, photocatalytic studies of Mo-doped TiO_2 films have been carried out by measuring the degradation of MB dye, which indicates the optimal degree of Mo doping in Mo/TiO_2 films.

2 | MATERIALS AND METHODS

Reactive RF magnetron sputtering was used to deposit TiO_2 and Mo-doped TiO_2 (Mo/TiO_2) thin films on glass and n-type silicon (100) substrates. The substrates were cleaned by employing standard cleaning methods and loaded into a process chamber. Before deposition, the chamber was evacuated to a pressure of 6×10^{-3} mbar by a rotary pump (Pfeiffer Vacuum, DUO 10 M, Germany) and then further evacuated to an ultimate pressure of 2.5×10^{-6} mbar by using a turbo molecular pump (Oerlikon, Turbovac 361C, Germany).

A Ti target with 99.99% purity and a 2-inch diameter, from Itasca, Korea, was utilized to prepare TiO_2 films. Rectangular 2 mm thick Mo (99.99%) strips of different lengths were placed on the Ti target surface to deposit the Mo/TiO_2 films. A constant distance of 50 mm was maintained between the target and substrate. The films were deposited at a constant power of 100 W and a process pressure of 10.2 mbar. In the chamber, the process pressure was maintained by using argon (99.99%) and oxygen (99.9%) at flow rates of 12 and

TABLE 1 Literature survey of deposition methods, conditions, band gaps, and photocatalytic properties of Mo/TiO2 films

Sl. No	Methods	Mo (at %)	Postannealing/Substrate Temperature (°C)	Phase	Band Gap (eV)	Degradation	References
1	DRMS	2.4-5.3	400-600	A	3.44-3.59	MB (60-70% in 5 h)	20
2	MEP	7.9-26.2	–	A	2.3-2.5	Toluene	21
3	SG	1–10	500 (5 h)	TiO_2	2.65-3.2	MB	16
4	SG	1-3	450 (2 h)	A	3.05-3.12	MO (73% in 2.5 h)	18
5	SG	5.12, 5.66, and 11.02	600	TiO_2	2.81-2.75	Tebuconazole pesticide	23
6	RMS	1 to 10 wt%	600 (1 h)	A	3.28-3.36	-	24
7	DRMS	0.9-3.6 wt%	550	A	3.7-3.2	MB	25
8	UMS	2.69-11.81	600	A, R, Am	-	MB	22
9	PDS	2.44-6.96	400 and 600	A	2.95-3.17	MB	26
10	SG	0.5-3.5	300-650	A	3.01-2.79	MB (36% efficiency)	27
11	*RRS*	*1.95-25.29 wt%*	*400*	*A*	*3.23-3.12*	*MB (59.6% at 1.5 h)*	*This paper*

DRMS indicates DC reactive magnetron sputtering; MEP, microemulsion preparation; SG, sol-gel; RMS, RF magnetron sputtering; UMS, unbalanced magnetron sputtering; PDS, pulsed DC sputtering; RRS, RF reactive sputtering; A, anatase; R, rutile; Am, amorphous; MB, methylene blue; MO, methyl orange.

3 sccm, respectively. Also, the deposition time and substrate temperature were kept constant at 60 minutes and 400°C. Presputtering was carried out for 10 to 20 minutes to remove the native oxide and surface contamination from both the target and the metallic Mo strips by using the same pressure and power as those were used for deposition. Mo strips of 1 × 5, 1 × 10, 1 × 15, and 1 × 20 mm^2 in width and length were used to develop the doped TiO_2 films.

2.1 | Characterization

The crystalline structure of deposited TiO_2 and Mo/TiO_2 films were analyzed in θ-2θ mode by using a 9 kW X-ray diffractometer (Rigaku, Japan). The samples were scanned with a step size of 0.02° and a scan rate of 3° $minutes^{-1}$. The morphology was studied by field emission scanning electron microscopy (FESEM) by using a Carl Zeiss Supra 55, and chemical composition was evaluated by an energy dispersive spectroscopy facility attached with FESEM. Charging of the sample was avoided by coating it with a few nanometers of gold for FESEM analysis. The roughness of the films was determined by using atomic force microscopy (AFM). The AFM topography was obtained with a drive frequency of 240 kHz and a force constant of 11.8 N m^{-1} in tapping mode.

X-ray photoelectron spectroscopy (XPS) was employed to study the elemental oxidation states and surface characteristics of TiO_2 and Mo-doped TiO_2 films by using a Thermo Scientific MultiLab 2000 spectrometer. Nonmonochromatic AlKα radiation (1486.6 eV) with an X-ray source operated at 150 W (15 kV, 10 mA) was used to investigate the deposited films. The C1s peak at 284.5 eV was taken as a reference to analyze the binding energies of deposited films. Thin film samples were mounted on sample holders after cutting into small pieces (10 mm × 10 mm) and kept in a preparation chamber at 1×10^{-8} Torr ultrahigh vacuum for 5 hours to remove volatile surface contamination. After 5 hours, the samples were transferred into analyzer chamber having ultrahigh vacuum of 1×10^{-9} Torr one by one. A pass energy of 40 eV with a step increment of 0.05 eV was used to obtain individual core level spectra, and survey spectra were obtained with a 70 eV pass energy and 0.5 eV step size.

The optical properties of TiO_2 and Mo/TiO_2 were studied by using a ultraviolet-visible spectrometer (JASCO 670, Japan). A Tauc extrapolation plot was used to calculate the optical band gap (E_o) of the films. The absorption coefficient was calculated by the following equation:

$$\alpha h\nu = A(E - E_o)^m$$

where E, E_o, m, h, A, and m are the energy of the incident photons, initial energy of the photons, frequency, Planck's constant, proportionality constant, and an integer, respectively.

2.2 | Photocatalytic studies

The photocatalytic activities of pristine TiO_2 and Mo/TiO_2 films were studied via photodegradation of a dilute MB solution (2 ppm concentration, M2661, Samchun Chemical, Suncheon, Korea). Methylene blue was chosen as a model organic compound. The MB solution was poured onto the pristine TiO_2 and $Mo\text{-}TiO_2$ films. The films were then irradiated under artificial sunlight from a Xenon arc lamp (Newport, Oriel Instruments, USA) equipped with an A.M. 1.5 filter, which had a light intensity of 100 mW cm^{-2}. The MB solution was collected after 1 hour 30 minutes, and the changes in MB concentration were estimated by measuring the intensity of the MB absorption peak at 664 nm using the ultraviolet-visible spectrometer (Optizen POP Mecasys Co. LTD, Korea). The tests were repeated to confirm the reliability of the results.

3 | RESULTS AND DISCUSSION

3.1 | Structural studies

The X-ray diffraction (XRD) patterns of TiO_2 and Mo/TiO_2 thin films on silicon (100) substrates are shown in Figure 1. The TiO_2 and doped TiO_2 films are polycrystalline with anatase phase, and they are well fitted with the tetragonal crystal structure. The XRD reflections of the films agree well with those of JCPDS file No. 21-1272. The peaks observed at 2θ of 25.28°, 37.80°, 48.04°, 53.89°, and 62.68° correspond to the (101), (004), (200), (105), and (204) planes, respectively. The intensity of the strong (101) peak decreases with increasing Mo dopant concentration, which may be due to changes in the mobility of the titanium and oxygen atoms. Moreover, the (101) peak gets broadened due to the microstrain produced by the slight mismatch in the size of Ti ion and Mo ion. Bregani et al[34] have observed larger microstrain when the Mo dopant concentration is increased. The crystalline nature of TiO_2 decreases while doping with molybdenum. From Figure 1, it is observed that as-deposited Mo/TiO_2 films with higher concentration of Mo tend to be amorphous in nature. This can be attributed to the inhibition of TiO_2 crystal growth by addition of molybdenum.[35] Increasing the concentration of Mo also leads to a reduction in the nucleation of the crystalline phase of anatase TiO_2.[36]

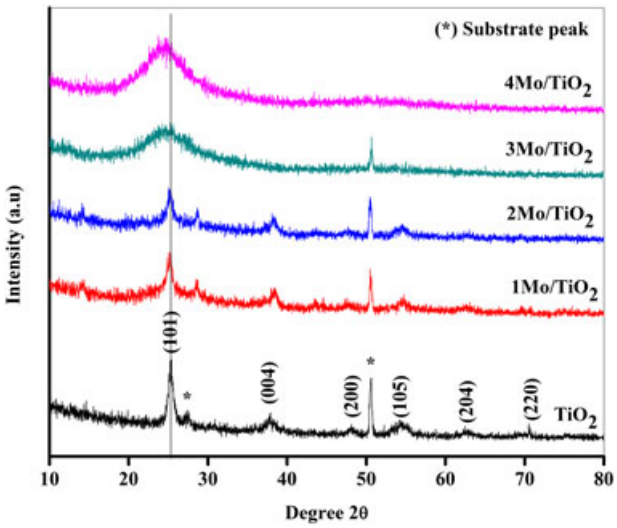

FIGURE 1 X-ray diffraction (XRD) patterns of various thin films on silicon substrate: A, TiO_2; B, $1Mo/TiO_2$; C, $2Mo/TiO_2$; D, $3Mo/TiO_2$; and E, $4Mo/TiO_2$

TiO_2 films with low Mo concentrations are found to be crystalline, and the films doped with more than 1.5 at.% Mo are amorphous. The crystallite sizes (C_s) of the films, summarized in Table 2, have been estimated by using Scherer's formula:

$$C_s = \frac{kL}{\beta cos\ \theta} \quad (1)$$

where k is the shape factor (0.9), β is the full width at half maximum of the peak, and L is the X-ray wavelength. Table 2 shows that the crystallite size of pure TiO_2 is ~6.3 Å, while the crystallite size of the Mo-doped TiO_2 films is higher than that of pure TiO_2 films (~118.4 Å). Houng et al[29] have also observed this increasing trend.

TABLE 2 Variation of crystallite size (C_s), dislocation density (δ), strain (ε), stack faulty probability (α), and stress (σ_{stress}) for pure TiO_2 and Mo-doped TiO_2 thin films

at.% of Mo	C_s (Å)	$\varepsilon \times 10^{-3}$	δ (lines/m)	α	σ_{stress} (GPa)
0.0 (TiO_2)	6.3	2.930	7.1×10^{15}	0.388	0.414
0.5 (1Mo/TiO_2)	118.3	2.930	2.5×10^{19}	0.379	0.414
1.5 (2Mo/TiO_2)	118.4	2.926	1.0×10^{20}	0.056	0.414

The lattice strains (ε) of the films have been calculated by using Equation 2:

$$\varepsilon = \frac{\beta \cos\theta}{4} \quad (2)$$

The lattice strain of the films is almost constant at ~2.9299×10^{-3} (Table 2). Dhanapandian et al[37] have observed a slightly high strain of 3.3663×10^{-3} in Sn-doped TiO_2 thin films.

The dislocation densities of the TiO_2 and Mo-doped TiO_2 have been calculated by using Equation 3:

$$\delta = \frac{1}{C_s} \quad (3)$$

The dislocation density of the films increases with the Mo dopant concentrations from 7.1×10^{15} to 1.0×10^{20} lines/m (Table 2), because of the difference in ionic radii of Ti and Mo ions. Similar results have been observed by Dhanapandian et al[37] when Sn is doped into TiO_2 for antibacterial applications.

The stress of the deposited films has been estimated by Equation 4:

$$\sigma_{stress} = \frac{\varepsilon}{2}E \quad (4)$$

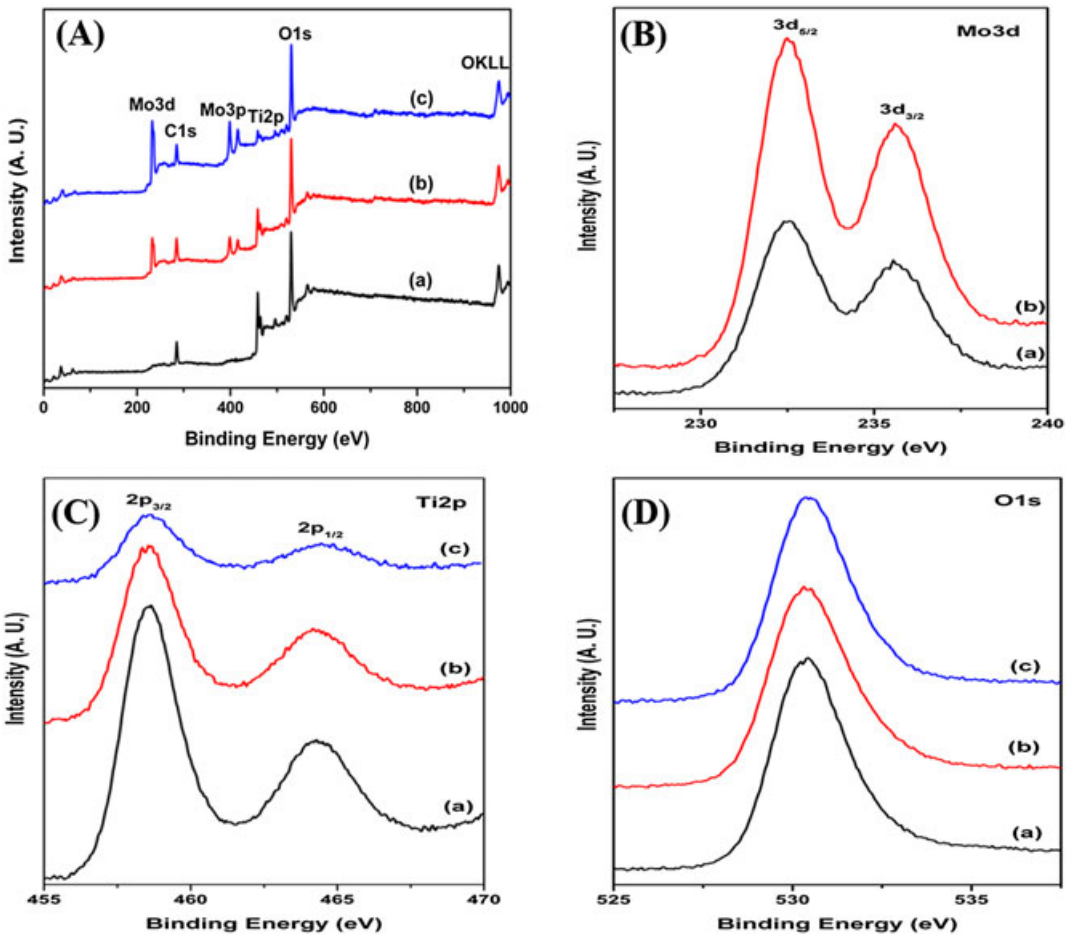

FIGURE 2 A, XPS survey spectra of: (a) TiO_2, (b) 1Mo/TiO_2, and (c) 4Mo/TiO_2; B, Mo3d core level spectra of (a) 1Mo/TiO_2 and (b) 4Mo/TiO_2; C, Ti2p core level spectra of (a) TiO_2, (b) 1Mo/TiO_2, and (c) 4Mo/TiO_2; and D, O1s core level spectra of (a) TiO_2, (b) 1Mo/TiO_2, and (c) 4Mo/TiO_2

where E is the Young's modulus of the material (282.76 GPa)[38] and ε is the strain of the films. The positive values indicate that the stress is in tensile nature. The observed stress in the films is almost constant at ~0.4142 GPa (Table 2) for both doped and undoped TiO_2 films. The observed values are much lower than that of the films developed by Raj et al[39] (0.763 GPa).

The stacking fault probability (α) has been estimated by Equation 5:

$$\alpha = \left[\frac{2\pi^2}{\left(45\sqrt{3}\tan\theta\right)}\right]\Delta(2\theta) \quad (5)$$

The stacking fault probability of the peaks has been calculated from the XRD peak shift of the films with reference to JCPDS file No: 21-1272 by using Equation 5. The faults vary from 0.0562 to 0.3876, and the TiO_2 film shows higher stacking fault value than the doped films. The maximum stacking fault of 0.3876 is shown by a pure TiO_2 thin film (Table 2).

3.2 | X-ray photoelectron spectroscopy studies

Detailed XPS characterization has been carried out to understand the nature of the surface of the Mo/TiO_2 thin films. X-ray photoelectron spectroscopy of TiO_2 has also been recorded for comparison. Typical XPS survey spectra of Mo/TiO_2 thin films with different compositions are shown in Figure 2A. The survey spectra clearly show the presence of Mo, Ti, and O species in the as-deposited films. The Mo3d core level spectra of Mo/TiO_2 thin films are shown in Figure 2B. The $Mo3d_{5/2,3/2}$ peaks observed at 232.5 and 235.6 eV are assigned to Mo^{6+} species.[40,41] The binding energy peak positions indicate that Mo exists in fully oxidized Mo^{6+} in the films. There is no signature of Mo^0 or other molybdenum suboxide species in the films. In the Ti2p core level spectra

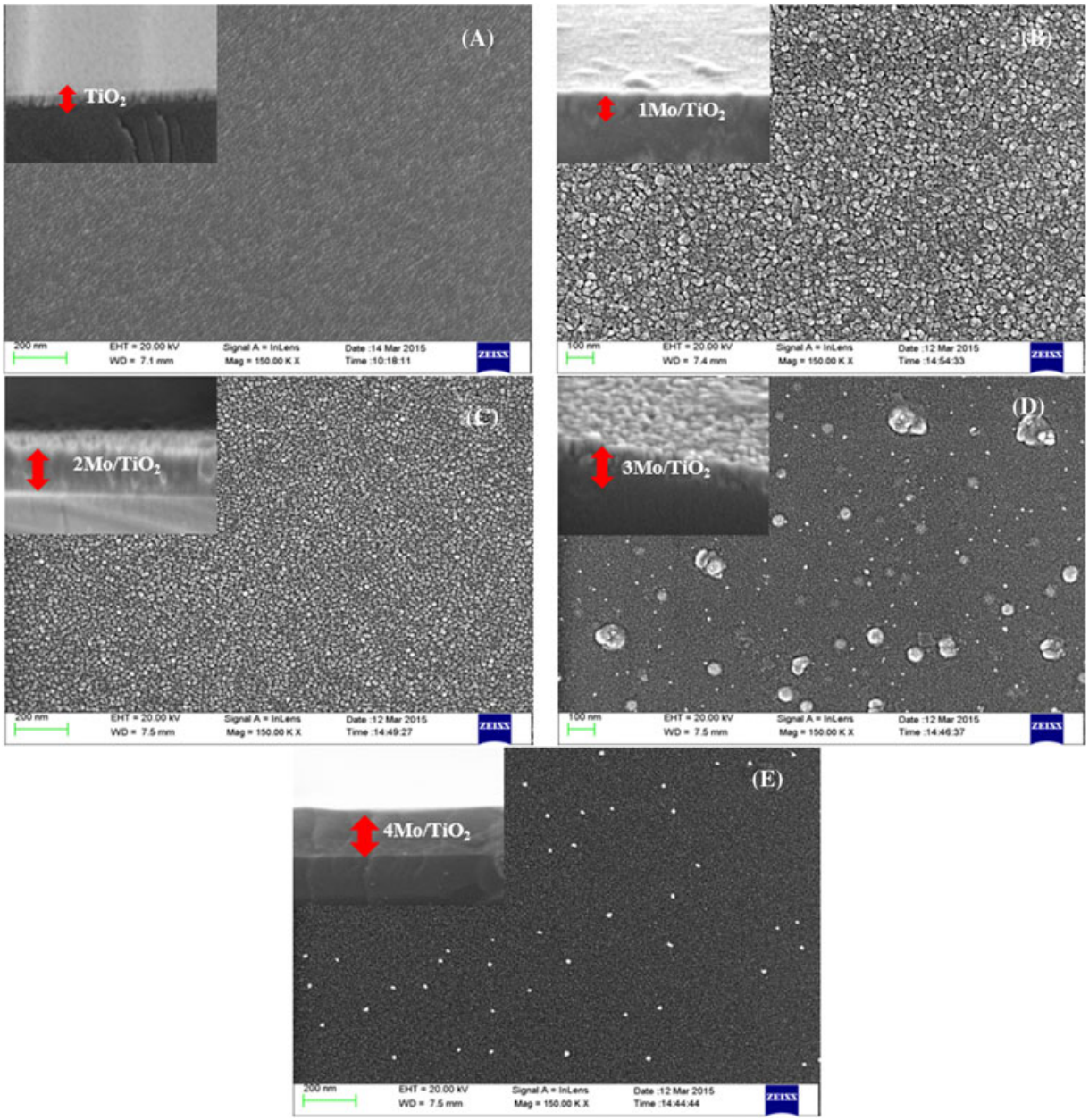

FIGURE 3 FESEM surface morphology and cross-sectional images (inset) of A, TiO_2; B, 1Mo/TiO_2; C, 2Mo/TiO_2; D, 3Mo/TiO_2; and E, 4Mo/TiO_2, and typical ED spectra of F, TiO_2 and G, Mo-doped TiO_2

shown in Figure 2C, the $2p_{3/2,1/2}$ peaks at 458.5 and 464.33 eV correspond to Ti^{4+} in TiO_2.[35] In Mo/TiO_2 films, the titanium is present in +4 oxidation state as in pure TiO_2, and the addition of Mo does not influence the nature of the Ti^{4+} species significantly. The O1s core level spectra of all films, shown in Figure 2D, contain a main peak at ~530.0 eV, which is attributed to oxide materials only.[35] The relative surface concentrations of Mo and Ti in the thin films are calculated from the integrated peak areas and atomic sensitivity factors of Mo3d and Ti2p. The surface concentrations of Ti and Mo are 58 and 42 at.% in $1Mo/TiO_2$ and 22.5 and 77.5 at.% in $4Mo/TiO_2$, respectively.

TABLE 3 The roughness and thickness of TiO_2 and Mo-doped TiO_2 thin films

Sample	R_a (nm)	R_{rms} (nm)	Thickness (nm)
TiO_2	0.106	0.156	53.02
$1Mo/TiO_2$	0.673	1.458	37.60
$2Mo/TiO_2$	0.169	0.216	58.77
$3Mo/TiO_2$	1.804	3.250	65.80
$4Mo/TiO_2$	0.129	0.171	117.7

3.3 | Morphological studies

The surface morphologies of the TiO_2 and Mo/TiO_2 films have been investigated by FESEM. Figure 3A–E shows FESEM images of pristine TiO_2 and Mo/TiO_2 films that are deposited on silicon substrates at a constant temperature of 400°C. The surface morphologies of the deposited films depend on the concentration of Mo dopants. The pristine and doped TiO_2 films show uniform spreading of grains and dense structures that cover the entire surface area of the silicon substrate without surface cracks or voids. Clear differences in particle size are observed between these films. The particle sizes in pristine TiO_2 thin films are ~7 Å. In contrast, the doped films have larger particle sizes of ~120 Å. These data correlate well with XRD measurements. The

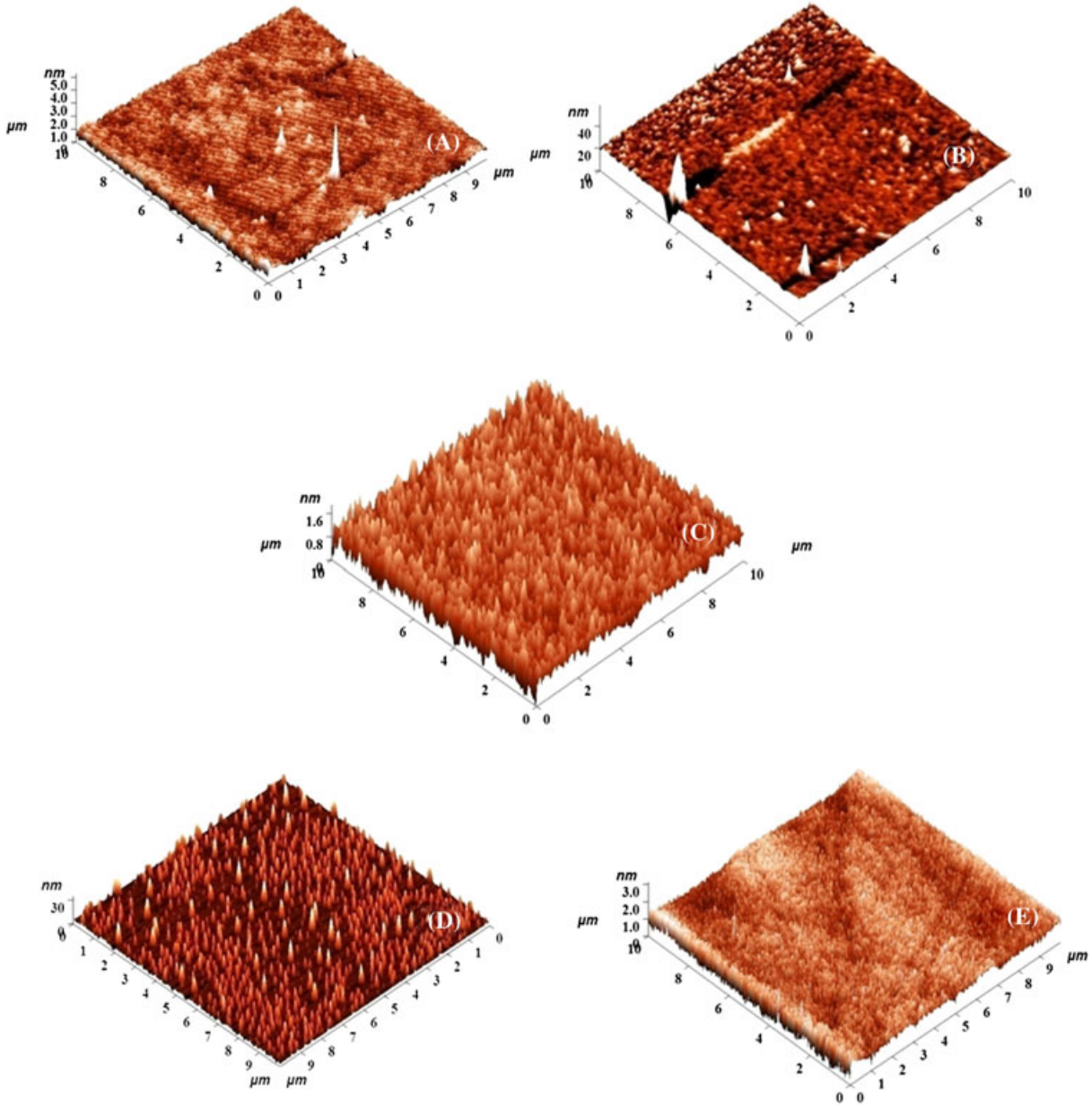

FIGURE 4 AFM images of A, TiO_2; B, $1Mo/TiO_2$; C, $2Mo/TiO_2$; D, $3Mo/TiO_2$; and E, $4Mo/TiO_2$

highly Mo-doped TiO_2 samples (Figure 3D: $3Mo/TiO_2$ and Figure 3E: $4Mo/TiO_2$) show bigger grains than the TiO_2 films with low concentrations of Mo dopants (Figure 3B: $1Mo/TiO_2$ and Figure 3C: $2Mo/TiO_2$). Overall, the grain sizes of Mo-doped TiO_2 films are larger than those of pristine TiO_2 films. Cross-sectional images of TiO_2 and Mo-doped TiO_2 films are shown in the inset of Figure 3. The films show good bonding to the silicon substrate. With the exception of $1Mo/TiO_2$ (Figure 3B) and $4Mo/TiO_2$ (Figure 3E), the films have a slightly columnar structure (Figure 3A–C). The thicknesses of the films increase from ~37 to ~117 nm with increasing Mo concentrations (Table 3).

Atomic force microscopy topographical images of the deposited pure TiO_2 and Mo-doped TiO_2 films are shown in Figure 4. The columnar structure is also observed in the 3D AFM images, which reveals that growth occurred in the (101) plane of the films. This finding agrees well with the XRD data. The estimated average roughness (R_a) and root-mean-square roughness (R_{rms}) values of the films are summarized in Table 3. R_a and R_{rms} are varied from 0.106 to 1.804 nm and from 0.156 to 3.250 nm, respectively. All the doped films have higher R_a and R_{rms} values than the pure TiO_2 films. However, the $3Mo/TiO_2$ sample shows the highest R_a and R_{rms} values compared to the other films.

3.4 | Optical properties

Figure 5A,B shows the transmittance and absorption spectra of the TiO_2 and Mo/TiO_2 films deposited on glass substrates at a substrate temperature of 400°C. The TiO_2 film shows an average transmittance of ~85% in the wavelength range of 300 to 1000 nm. Similar transmittance behavior is also observed in the Mo-doped TiO_2 films. The Mo concentration does not significantly affect the film transmittance. The absorption spectra in Figure 5B reveal that the absorption edges of Mo-doped films are shifted toward a higher wavelength (red shift) compared to the pure TiO_2 film; the edge is shifted toward higher wavelength with increasing Mo concentrations.[30] The absorption edges of doped films are in the range of 350 to 420 nm. The transmittance spectra are used to evaluate the band gap of TiO_2 and Mo-doped TiO_2 films. The indirect band gaps of TiO_2 and Mo-doped TiO_2 films are determined by plotting $\alpha^{1/2}$ versus the photon energy ($h\nu$)[42] as shown in Figure 5C. The observed band gap of TiO_2 matches well with the literature (~3.27 eV).[36] The band gaps of the Mo-doped TiO_2 films vary from ~3.23 to ~3.12 eV and are lower than the band gap of the pure TiO_2 film. The band gaps of TiO_2 films decrease with increasing Mo dopant concentrations; the lowest band gap (~3.12 eV) is observed in the $4Mo/TiO_2$ sample.

3.5 | Photocatalytic activity

The photocatalytic activities of TiO_2 and Mo/TiO_2 thin films have been studied by using MB dye degradation. The decomposition of MB under visible light has been measured after 1.5 hours of irradiation. The absorption spectra of samples with different Mo concentrations are measured during MB degradation, and the results are displayed in Figure 5D. Methylene blue degradation has been measured by using

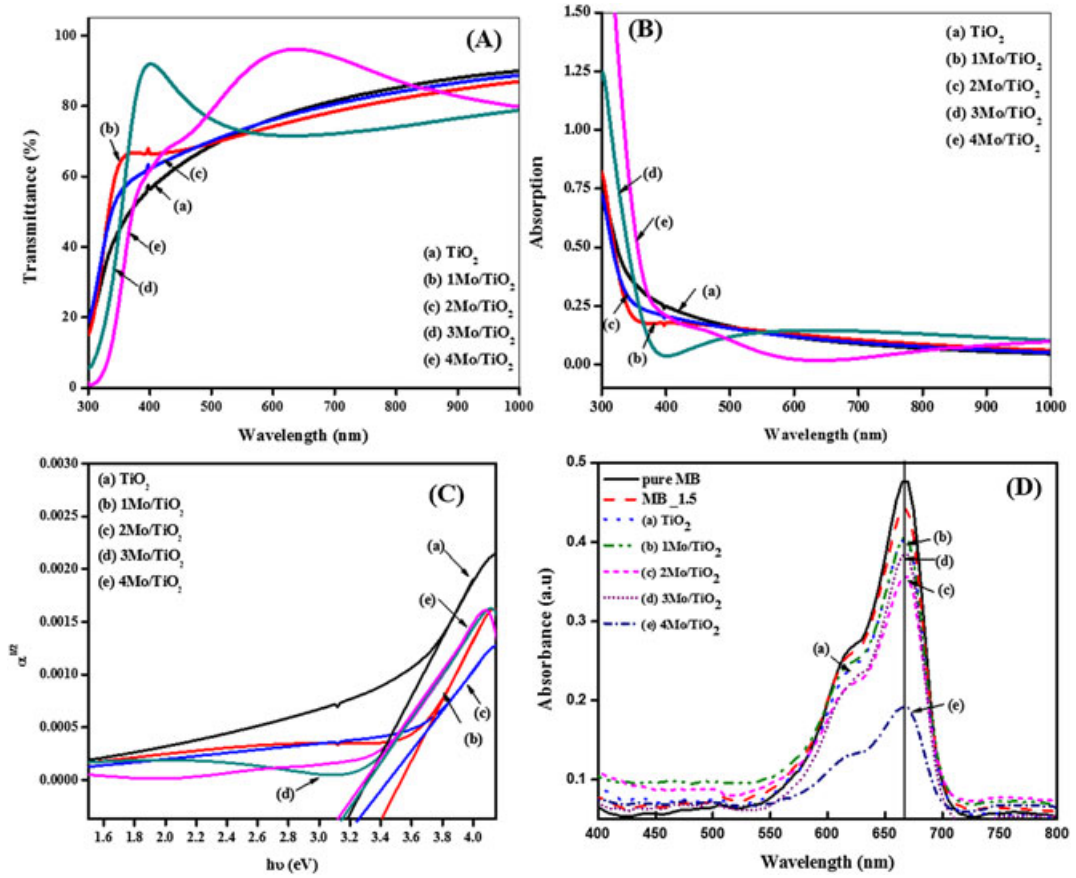

FIGURE 5 A, Transmittance; B, absorption spectra of deposited thin films on glass with various compositions; C, variation of $\alpha^{1/2}$ versus photon energy ($h\nu$) of deposited thin films; and D, absorption spectra of MB degradation of thin films

TABLE 4 The degradation efficiency of TiO_2 and Mo-doped TiO_2 films

Sample Details	Degradation Efficiency [%] Test 2
Pure MB	–
Photolysis of MB 1.5 h	7.1
TiO_2	15.5
$1Mo/TiO_2$	14.9
$2\ Mo/TiO_2$	25.4
$3Mo/TiO_2$	19.53
$4\ Mo/TiO_2$	59.6

the change in absorbance of MB at 664 nm. In the absence of a catalytic film, the degradation of MB is negligible. Without Mo, the TiO_2 film shows minimal photodegradation (15%), while ~59.6% degradation occurs with the 4 at.% Mo-doped TiO_2 thin film.

The reaction mechanism of photocatalytic degradation of MB is presented in Equation 6.

$$MB + Mo{:}TiO_2 \xrightarrow{hv(UVA)} CO_2 + H_2O + NO_3 + NH_4^+ + SO_4^{2-} + Mo{:}TiO_2 \quad (6)$$

The absorption edge of the $Mo^{5+/6+}$-doped TiO_2 is extended to the visible light region, causing increased photocatalytic activity in the visible region. Doping with Mo also increases the number of carrier electrons, resulting in faster reaction kinetics because of superoxide radical formation. These hydroxyl and superoxide radicals can react with MB to yield degradation products. The degradation efficiency of samples after 2 tests is presented in Table 4.

4 | CONCLUSIONS

Reactive RF magnetron sputtering has been used to deposit TiO_2 and Mo-doped TiO_2 thin films on glass and silicon substrates at a substrate temperature of 400°C. The XRD patterns reveal a (101) orientation; thus, the films show the tetragonal structure of anatase TiO_2. The crystalline structure and optical band gaps of the films decrease with increasing Mo concentrations. A constant stress of ~0.4142 GPa is observed in both doped and undoped TiO_2 films. XPS results demonstrate the presence of Mo^{6+} species in all the deposited Mo/TiO_2 films. All the doped films have higher R_a and R_{rms} compared to pure TiO_2 films, with values in the ranges of 0.106 to 1.804 nm and 0.156 to 3.250 nm, respectively. The transmittance spectra of Mo-doped TiO_2 films show redshift. The highest degree of dye degradation is seen with the $4Mo/TiO_2$ film.

ACKNOWLEDGEMENT

This work was supported by the National Research Foundation of Korea (NRF) grant funded by the Korean Government (MSIP) (no. 2015R1C1A2A01052256).

ORCID

I. Neelakanta Reddy http://orcid.org/0000-0003-2713-962X
Parthasarathi Bera http://orcid.org/0000-0001-6173-6263

REFERENCES

1. Kubacka A, Fernández-García M, Colón G. Advanced nanoarchitectures for solar photocatalytic applications. *Chem Rev*. 2012;112(3):1555-1614. https://doi.org/10.1021/cr100454n
2. Nair PB, Justinvictor VB, Daniel GP, Joy K, Ramakrishnan V, Thomas PV. Effect of RF power and sputtering pressure on the structural and optical properties of TiO_2 thin films prepared by RF magnetron sputtering. *Appl Surf Sci*. 2011;257(24):10869-10875. https://doi.org/10.1016/j.apsusc.2011.07.125
3. Shahmoradi B, Ibrahim IA, Sakamoto N, et al. In situsurface modification of molybdenum-doped organic–inorganic hybrid TiO_2nanoparticles under hydrothermal conditions and treatment of pharmaceutical effluent. *Environ Technol*. 2010;31(11):1213-1220. https://doi.org/10.1080/09593331003592261
4. Du Y, Gan Y, Yang P, Cuie Z, Hua N. Cyclic voltammetry and contact angle measurement studies of the Mo(VI) ions doped TiO2 thin films. *Mater Chem Phys*. 2007;103(2-3):446-449. https://doi.org/10.1016/j.matchemphys.2007.02.063
5. Linsebigler AL, Lu G, Yates JT. Photocatalysis on TiO_2 surfaces: Principles, mechanisms, and selected results. *Chem Rev*. 1995;95(3):735-758. https://doi.org/10.1021/cr00035a013
6. Hoffman MR, Martin ST, Choi W, Bahneman DW. Environmental applications of semiconductor photocatalysis. *Chem Rev*. 1995;95(1):69-96. https://doi.org/10.1021/cr00033a004
7. Cohen MM. *Introduction to the theory of semiconductors*. Amsterdam: Gordon; 1999.
8. Ranjit KT, Viswanathan B. Synthesis, characterization and photocatalytic properties of iron-doped TiO_2 catalysts. *J Photochem Photobiol A Chem*. 1997;108(1):79-84. https://doi.org/10.1016/S1010-6030(97)00005-1
9. Huo Y, Zhu J, Li J, Li G, Li H. An active La/TiO_2 photocatalyst prepared by ultrasonication-assisted sol–gel method followed by treatment under supercritical conditions. *J Mol Catal A Chem*. 2007;278(1-2):237-243. https://doi.org/10.1016/j.molcata.2007.07.054
10. Liu Z, Guo B, Hong L, Jiang H. Preparation and characterization of cerium oxide doped TiO_2 nanoparticles. *J Phys Chem Solid*. 2005;66(1):161-167. https://doi.org/10.1016/j.jpcs.2004.09.002
11. Asahi R. Visible-light photocatalysis in nitrogen-doped titanium oxides. *Science*. 2001;293(5528):269-271. https://doi.org/10.1126/science.1061051
12. Sathish M, Viswanathan B, Viswanath RP, Gopinath CS. Synthesis, characterization, electronic structure, and photocatalytic activity of nitrogen-doped TiO_2 nanocatalyst. *Chem Mater*. 2005;17(25):6349-6353. https://doi.org/10.1021/cm052047v
13. Sakthivel S, Kisch H. Daylight photocatalysis by carbon-modified titanium dioxide. *Angew Chem Int Ed*. 2003;42(40):4908-4911. https://doi.org/10.1002/anie.200351577
14. Xiao Q, Zhang J, Xiao C, Si Z, Tan X. Solar photocatalytic degradation of methylene blue in carbon-doped TiO_2 nanoparticles suspension. *Sol Energy*. 2008;82(8):706-713. https://doi.org/10.1016/j.solener.2008.02.006
15. Wang X, Meng S, Zhang X, Wang H, Zhong W, Du Q. Multi-type carbon doping of TiO_2 photocatalyst. *Chem Phys Lett*. 2007;444(4-6):292-296. https://doi.org/10.1016/j.cplett.2007.07.026
16. Yu CJ, Yu J, Ho W, Jiang Z, Zhang L. Effects of F-doping on the photocatalytic activity and microstructures of nanocrystalline TiO_2 powders. *Chem Mater*. 2002;14(9):3808-3816. https://doi.org/10.1021/cm020027c
17. Wang Y, Zhang R, Li J, Li L, Lin S. First-principles study on transition metal-doped anatase TiO_2. *Nanoscale Res Lett*. 2014;9(1):46. https://doi.org/10.1186/1556-276X-9-46
18. Kubacka A, Colón G, García MF. Cationic (V, Mo, Nb, W) doping of TiO_2–anatase: A real alternative for visible light-driven photocatalysts. *Catalysis Today*. 2009;143(3-4):286-292. https://doi.org/10.1016/j.cattod.2008.09.028

19. Majeed J, Nayak C, Jha SN, Bhattacharyya K, Bhattacharyya D, Tripathi AK. Correlation of Mo dopant and photocatalytic properties of Mo incorporated TiO_2: An EXAFS and photocatalytic study. *RSC Adv*. 2015;5(110):90932-90940. https://doi.org/10.1039/C5RA14613E
20. Vomiero A, Della Mea G, Ferroni M, et al. Preparation and microstructural characterization of nanosized Mo–TiO_2 and Mo–W–O thin films by sputtering: Tailoring of composition and porosity by thermal treatment. *Mater Sci Eng B Solid-State Mater Adv Technol*. 2003;101 (1-3):216-221. https://doi.org/10.1016/S0921-5107(02)00666-9
21. Wang S, Bai LN, Sun HM, Jiang Q, Lian JS. Structure and photocatalytic property of Mo-doped TiO2 nanoparticles. *Powder Technol*. 2013; 244:9-15. https://doi.org/10.1016/j.powtec.2013.03.054
22. Mardare D, Cornei N, Luca D, et al. Synthesis and hydrophilic properties of Mo doped TiO_2 thin films. *J Appl Phys*. 2014;115(21):213501. https://doi.org/10.1063/1.4880339
23. Fisher L, Ostovapour S, Kelly P, et al. Molybdenum doped titanium dioxide photocatalytic coatings for use as hygienic surfaces: the effect of soiling on antimicrobial activity. *Biofouling*. 2014;30(8):911-919. https://doi.org/10.1080/08927014.2014.939959
24. Kelly P, West G, Ratova M, Fisher L, Ostovarpour S, Verran J. Structural formation and photocatalytic activity of magnetron sputtered titania and doped-titania coatings. *Molecules*. 2014;19(10):16327-16348. https://doi.org/10.3390/molecules191016327
25. Huang J-g, Guo X-t, Wang B, et al. Synthesis and photocatalytic activity of Mo-doped TiO_2 nanoparticles. *J Spectrosc*. 2015; 681850. http://doi.org/10.1155/2015/681850
26. Ratova M, Kelly PJ, West GT, Iordanova I. Enhanced properties of magnetron sputtered photocatalytic coatings via transition metal doping. *Surf Coat Technol*. 2013;228:S544-S549. https://doi.org/10.1016/j.surfcoat.2012.04.037
27. Kubacka A, Colón G, Fernández-García M. Cationic (V, Mo, Nb, W) doping of TiO_2–anatase: A real alternative for visible light-driven photocatalysts. *Catal Today*. 2009;143(3-4):286-292. https://doi.org/10.1016/j.cattod.2008.09.028
28. Devi LG, Murthy BN. Characterization of Mo doped TiO_2 and its enhanced photo catalytic activity under visible light. *Catal Lett*. 2008; 125(3-4):320-330. https://doi.org/10.1007/s10562-008-9568-4
29. Houng B, Liu CC, Hung MT. Structural, electrical and optical properties of molybdenum-doped TiO_2 thin films. *Ceram Int*. 2012;39:3669-3676. https://doi.org/10.1016/j.ceramint.2012.10.197
30. Luo SY, Yan BX, Shen J. Enhancement of photoelectric and photocatalytic activities: Mo doped TiO_2 thin films deposited by sputtering. *Thin Solid Films*. 2012;522:361-365. https://doi.org/10.1016/j.tsf.2012.07.121
31. Li C, Zhang D, Jiang Z, Yao Z, Jia F. Mo-doped titania films: Preparation, characterization and application for splitting water. *New J Chem*. 2011;35(2):423-429. https://doi.org/10.1039/C0NJ00409J
32. Li M, Zhang J, Zhang Y. Electronic structure and photocatalytic activity of N/Mo doped anatase TiO2. *Cat Com*. 2012;29:175-179. https://doi.org/10.1016/j.catcom.2012.10.014
33. Devi LG, Murthy BN, Kumar SG. Photocatalytic activity of V5+, Mo6+ and Th4+ doped polycrystalline TiO2 for the degradation of chlorpyrifos under UV/solar light. *J Mol Catal A Chem*. 2009;308(1-2):174-181. https://doi.org/10.1016/j.molcata.2009.04.007
34. Bregani F, Casale C, Depero LE, et al. Temperature effects on the size of anatase crystallites in Mo瑟TiO_2 and W瑟TiO_2 powders. *Sens Actuators B*. 1996;31(1-2):25-28. https://doi.org/10.1016/0925-4005(96)#80011-6
35. Sreedhar M, Reddy IN, Bera P, et al. Cu/TiO_2 thin films prepared by reactive RF magnetron sputtering. *Appl Phys A*. 2015;120(2):765-773. https://doi.org/10.1007/s00339-015-9254-5
36. Nejand BA, Sanjabi S, Ahmadi V. Optical and photocatalytic characteristics of nitrogen doped TiO_2 thin film deposited by magnetron sputtering. *Trans F: Nanotechnol*. 2010;17:102-107.
37. Dhanapandian S, Arunachalam A, Manoharan C. Highly oriented and physical properties of sprayed anatase Sn-doped TiO_2 thin films with an enhanced antibacterial activity. *Appl Nanosci*. 2015;6:387-397. https://doi.org/10.1007/s13204-015-0450-6
38. Solomon DH, Hawthorne DG. *Chemistry of pigments and fillers*. New York: Wiley; 1983.
39. Raj AME, Agnes V, Jothy VB, et al. Spray deposition and property analysis of anatase phase titania (TiO_2) nanostructures. *Thin Solid Films*. 2010;519(1):129-135. https://doi.org/10.1016/j.tsf.2010.07.073
40. Xu J, Tao J, Jiang S, Xu Z. Investigation on corrosion and wear behaviors of nanoparticles reinforced Ni-based composite alloying layer. *Appl Surf Sci*. 2008;254(13):4036-4043. https://doi.org/10.1016/j.apsusc.2007.12.039
41. Castañeda SI, Montero I, Ripalda JM, Diaz N, Galán L, Rueda F. X-ray photoelectron spectroscopy study of low-temperature molybdenum oxidation process. *J Appl Phys*. 1999;85(12):8415-8418. https://doi.org/10.1063/1.370690
42. Reddy IN, Reddy VR, Sridhara N, et al. Pulsed rf magnetron sputtered alumina thin films. *Ceram Int*. 2014;40(7):9571-9582. https://doi.org/10.1016/j.ceramint.2014.02.032

How to cite this article: Sreedhar M, Brijitta J, Reddy IN, et al. Dye degradation studies of Mo-doped TiO_2 thin films developed by reactive sputtering. *Surf Interface Anal*. 2018;50: 171–179. https://doi.org/10.1002/sia.6355